

Quantum Machine Learning for Photovoltaic Topology Optimization

Glen S Uehara
SenSIP Center, School of ECEE
Arizona State University
Tempe, AZ U.S.A.
guchara@asu.edu

Vivek Narayanaswamy
SenSIP Center, School of ECEE
Arizona State University
Tempe, AZ U.S.A.
vnaray29@asu.edu

Cihan Tepedelenlioglu
SenSIP Center, School of ECEE
Arizona State University
Tempe, AZ U.S.A.
cihan@asu.edu

Andreas Spanias
SenSIP Center, School of ECEE
Arizona State University
Tempe, AZ U.S.A.
spanias@asu.edu

Abstract—Photovoltaic array topology optimization was shown to improve efficiency in renewable energy plants. Previous studies demonstrated improvements via simulation at the level of 7-12% or more. In this paper, we describe solar array topology optimization systems based on quantum machine learning algorithms. The idea of using quantum machine learning can be useful in cases where the objective is to optimize power output in large sites with several thousands of panels. We specifically propose and assess a quantum circuit for a neural network implementation for photovoltaic topology optimization. Results and comparisons are presented using classical and quantum neural network implementations. In addition, solar array topology optimization simulations and comparisons using a quantum neural network are described for different numbers of qubits.

I. INTRODUCTION

Sensors and signal processing have been previously used for fault detection, topology optimization, and shading prediction [1]–[9]. Sensors typically monitor the voltage (V), current (I), irradiance, and temperature of each solar panel in a photovoltaic (PV) array [10]. It was shown that real-time solar array monitoring and control of a utility-scale PV array can be accomplished by smart monitoring devices (SMDs) [11]. The SMD (Fig. 1) has sensors, actuators (relays), a microprocessor, and an RF unit to transfer data to servers and the Internet for analytics.

Signal processing and machine learning (ML) algorithms can be used along with SMD measurements to detect faults, reconfigure connections, and predict shading. In fact, internet-connected SMDs attached to PV panels enable remote operators to manage the solar array as an Internet of Things (IoT) system [12].



Fig. 1 The smart monitoring device (SMD) for solar panel monitoring and control.

Machine learning for PV array management has been studied in [5], [11], [13]–[15]. In addition, a study on using

quantum computing methods for PV fault detection was reported in [16]. In particular, hybrid quantum neural networks were designed for PV fault detection [17]. The motivation for quantum machine learning solutions is to address PV analytics in situations involving multiple large-scale solar energy plants with thousands of PV panels.

In this paper, we study quantum machine learning algorithms for solar array topology optimization. We study specifically quantum neural network (QNN) solutions for optimizing the power output by switching across PV connection topologies. We design custom QNN circuits for use in dynamic topology switching. Our study is carried out at the simulation level and considers switching across two 3x4 topologies, namely series-parallel (SP) and total cross tied (TCT). Results from the QNN simulations are obtained for different numbers of qubits. QNN and classical NN are compared, and results are provided in terms of confusion matrices.

The overall system diagram used for PV monitoring and topology reconfiguration is shown in Fig. 2, SMDs installed on each solar panel provide voltage, current, and temperature data which is being used for analytics and PV array control. In addition, these devices have relays and can form connection topologies that can be switched upon instruction from an operator or an algorithm.

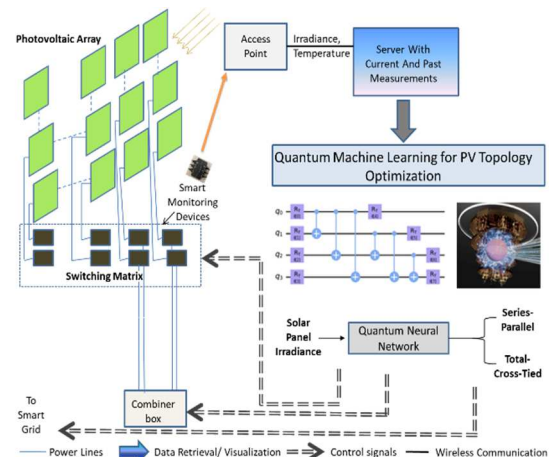


Fig. 2 Smart solar array monitoring system integrated with quantum machine learning topology reconfiguration algorithms.

The rest of the paper is organized as follows. Section II describes classical ML methods for topology optimization. Section III presents the implementation of NN using quantum computing and Section IV presents concluding remarks.

II. CLASSICAL ML FOR TOPOLOGY OPTIMIZATION

Partial shading on solar panels can detrimentally affect the power output from PV arrays. It was shown that PV topology reconfiguration is a viable method for improving the power output under shaded conditions [1].

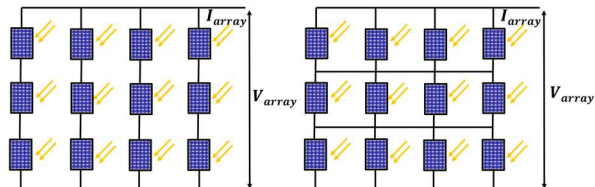


Fig. 3 Solar array connection topologies used in our study: a) on the left, the 3 x 4 series parallel (S-P), and b) on the right the 3 x 4 total cross tied (TCT) array configurations.

At a high level, topology reconfiguration involves switching the electrical connections between the panels based on input control signals. Various methods of reconnecting the panels have been proposed in [1], [2] to maximize the PV array output. In general, PV arrays are connected in the SP topology consisting of strings of panels connected in parallel. Additionally, it has been shown in [2] that significant power improvements can be obtained when the array is connected in a cross-tied manner, for e.g., TCT array. In the TCT topology (Fig. 3), every row consists of PV modules connected in parallel, and the resultant rows are connected in series. We note that these two topologies behave identically under perfect irradiance conditions. However, when there are mismatches and partial shading, one of the topologies can outperform the other in terms of power production. This naturally motivates the use of a ‘smart’ algorithm that automatically reconfigures the array into one of the topologies based upon the extent of shading or panel level irradiances. In this context, ML for topology reconfiguration has emerged as a popular approach and the authors of this paper have provided preliminary results in [6]. ML models, in particular, neural networks (NN) learn different patterns of the PV panel irradiances and predict the optimum configuration. Importantly, the use of ML for this application produces an end-to-end system that learns a function to directly map irradiances to the optimal topology.

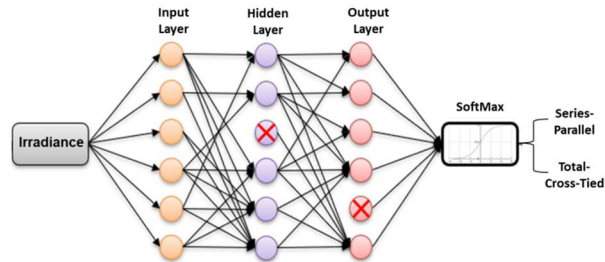


Fig. 4 Classical neural network for performing topology reconfiguration used in our study. The model produces an end-to-end mapping between irradiance and the optimal topology.

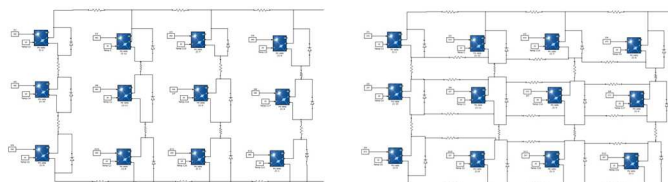


Fig. 5 MATLAB Simulink models for generating synthetic data: a) on the left, the 3 x 4 Series Parallel (S-P), and b) on the right, the 3 x 4 Total Cross Tied (TCT) array configurations.

Fig. 4 provides a functional diagram of the classical NN which can be used for topology reconfiguration. The following subsections describe the synthetic data generation process for training the neural network and the preliminary results.

A. Synthetic Data Generation for Topology Optimization

In this paper, we consider 3 x 4 PV arrays for data generation. Synthetic irradiance values for every panel of the 3 x 4 array have been generated using a binary mapping rule which is described in [6]. Basically, we assigned ‘0’ to a panel that is unshaded and ‘1’ to a shaded panel and populated 4096 irradiance profiles. The irradiance profiles are drawn from the uniform distribution. The uniform distribution is sampled for randomly chosen binary assignments and generates over 5000 instances of partial shading profiles. The topology reconfiguration can be viewed as a supervised learning problem that requires a completely labeled dataset with 5000 irradiance profiles for 12 PV panels (3x4 arrays). The label vector y is generated by passing every irradiance instance at a constant temperature of 27°C to a Simulink 3 x 4 Series SP and TCT (Fig. 3, 4) arrays and then we compare the maximum power generated.

B. Results using a Classical Neural Network

To perform PV topology reconfiguration, we trained a NN with three layers of 150 neurons each. The entire synthetic dataset was divided into the training and test set with a ratio of 70:30 respectively. The NN was trained for 150 epochs with a learning rate of 0.0001. When the trained NN was evaluated on the test set we obtain a test accuracy ~95%. Improvement in output power based on dynamic topology reconfiguration was estimated by calculation to be ~7%. In the next section a Quantum computing (QC) implementations are presented.

III. HYBRID QUANTUM NN FOR TOPOLOGY RECONFIGURATION

In our previous work [17], a hybrid Quantum Neural Network (QNN) (Fig. 6) was designed for PV fault detection. The hybrid QNN [18] system was designed and modeled using a state vector simulation [19].

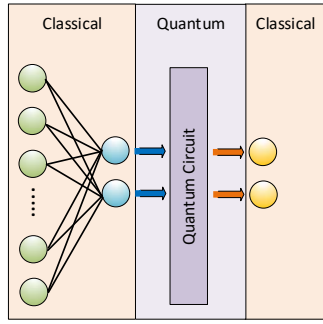


Fig. 6 Hybrid quantum-classical neural network architecture used for fault detection [17].

As observed in Table 1, we previously [17] examined various epochs and qubit choices to determine whether there were advantages in accuracy for fault detection. The results of our previous studies yielded an accuracy of about 90%, which was very encouraging. Motivated by previous results of Table 1, we launched a study of topology optimization, which we present in this paper.

TABLE 1. PREVIOUS FAULT DETECTION RESULTS AND COMPARISONS [17]

Fault Detection Algorithm	Training Epoch	Detection Accuracy
Classical NN	300	95.39%
Hybrid QNN1 (2 qubits)	25	87.8%
Hybrid QNN1 (2 qubits),	100	93.89%
Hybrid QNN1 (4 qubits),	25	90.2%
Hybrid QNN2 (2 qubits)	18	90.5%

Our study will again explore the hybrid QNN model and create an updated quantum circuit for topology optimization.

A. The Circuit-Centric Classification Model

We present a recently proposed model based on circuit-centric classification [20] for designing a hybrid QNN. This model is built using a three-step process, as shown in Fig. 7.

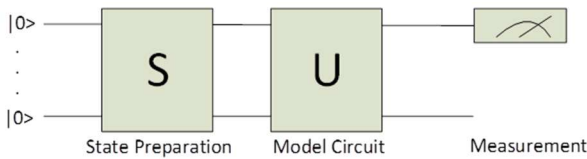


Fig. 7 Circuit-Centric design for new hybrid QNN based on the model circuit from [20].

First, the system prepares the data by performing a state preparation (S) by organizing the classical data into qubits to run the quantum circuit. Next, the qubits are processed through a model circuit, relying on a basic Unitary transform (U). Finally, qubit measurements are taken and transformed to binary data.

B. Hybrid QNN with Circuit-Centric model

With the most recent quantum circuit approach described in [20], a new hybrid quantum-classical neural network is

designed. This design also allows the addition of additional NN layers for topology optimization. To simulate the QNN, we used PennyLane [21] and the circuit-centric model is shown in Fig. 8.

$$\begin{aligned}
 0: & \text{---RX}(1.00)\text{---Rot}(0.24,0.89,0.08)\text{---} \rho\text{C} \text{---} \rho\text{X} \text{---} \langle Z \rangle \\
 1: & \text{---RX}(2.00)\text{---Rot}(0.28,0.22,0.73)\text{---} \rho\text{X} \text{---} \rho\text{C} \text{---} | \text{---} \langle Z \rangle \\
 2: & \text{---RX}(3.00)\text{---Rot}(0.83,0.29,0.63)\text{---} \rho\text{X} \text{---} \rho\text{C} \text{---} | \text{---} \langle Z \rangle \\
 3: & \text{---RX}(4.00)\text{---Rot}(0.31,0.93,0.44)\text{---} \rho\text{X} \text{---} \rho\text{C} \text{---} | \text{---} \langle Z \rangle
 \end{aligned}$$

Fig. 8 Circuit centric model [20] based on angle embedded and strongly entangled unitary matrix (e.g. 4 qubit with 1 layer).

The circuit example in Fig.8 prepares the input data into four qubits by angle embedding of the classical data. A unitary transform of the circuit is used and this consists of a rotation gate (*Rot*) with each qubits being entangled. We define *Rot*, Eq. (1), as an arbitrary single-qubit rotation where the weights are those used when training our system.

$$R(\phi, \theta, \omega) = RZ(\omega)RY(\theta)RZ(\phi) = \begin{bmatrix} e^{-j(\phi+\omega)/2} \cos(\theta/2) & -e^{-j(\phi-\omega)/2} \sin(\theta/2) \\ e^{-j(\phi-\omega)/2} \sin(\theta/2) & e^{j(\phi+\omega)/2} \cos(\theta/2) \end{bmatrix} \quad (1)$$

The circuit is updated by adding the strongly entangled unitary matrix gate when adding additional layers. This set of gates is repeated at each additional layer. This is represented in the *Rot* and the representation of the entanglement, as shown in Fig. 9.

C. Simulation Results

We use the same synthetic dataset generated for the classical NN as shown in the previous section. As stated earlier, the synthetic irradiance values for every panel of the 3 x 4 array were generated using a binary mapping rule described in [6], i.e., a “0” is assigned to an unshaded panel and “1” to a shaded panel. A total of 4096 irradiance profiles are generated for training. For the hybrid QNN simulation, the system determines whether we have the proper selection of unshaded or shaded panels. For the simulations, accuracy is defined as the process of correctly selecting the best panel topology, i.e., the one that will produce maximum power for a given shading pattern. Lastly, in the quantum implementations, the entire synthetic dataset was divided into training and test sets with a ratio of 70:30, respectively.

Fig. 10 [A] shows the accuracy of correctly selecting the best panel topology for a two qubit simulation with different numbers of layers. The figure shows that QNN has an accurate prediction of 80% as the number of layers increases. Fig. 10 [B] examines the same test but with four qubits. In this case, the simulations show that the accuracy predicts in the range of 82 to 85%. Finally, we select one of the simulations and form and report a confusion matrix. In Fig. 11, we observe that for a four qubit – one-layer system, we have an accuracy of panel selection of 85.12%. The results of the simulation are tabulated in Table 2.

$$0: \text{---RX}(1.00)\text{---Rot}(0.77,0.63,0.14)\text{---}rC\text{---}rX\text{---Rot}(0.04,0.69,0.19)\text{---}rC\text{---}rX\text{---}| \langle Z \rangle$$

$$1: \text{---RX}(2.00)\text{---Rot}(0.38,0.40,0.82)\text{---}lX\text{---}lC\text{---Rot}(0.35,0.59,0.90)\text{---}lX\text{---}lC\text{---}| \langle Z \rangle$$

Fig. 9 Circuit centric model [20] based on angle embedded and strongly entangled unitary matrix (2 qubit with 2 layer).

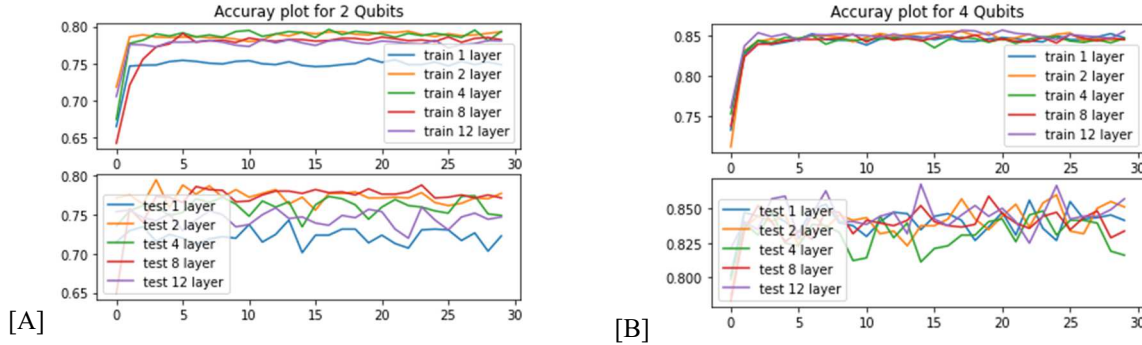


Fig. 10 New hybrid QNN training and testing accuracy of selecting the correct panel [A] Two qubit Training and Testing with different layers (1, 2, 4, 8, 12) [B] Four qubit Training and Testing with different layers (1, 2, 4, 8, 12).

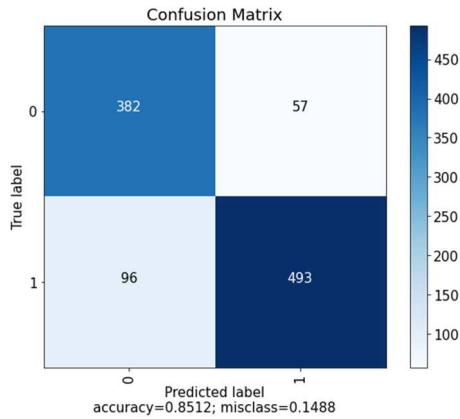


Fig. 11 Hybrid QNN confusion matrix showing 85.12% accuracy for panel selection on the topology optimization.

We now examine how the number of layers and the qubits affects the accuracy of the new hybrid QNN with model circuit design. As we can see in Table 2, the changes in the number of layers at four qubits were minimal. However, in two qubits systems, we observe that we do require at least four layers to reach over 75% accuracy of panel selection.. Furthermore, the simpler circuit only needs four qubits, one layer, and 30 epochs to reach 85% accuracy.

TABLE 2 QNN TOPOLOGY RECONFIGURATION COMPARISON

Number of Layers	Training		Validation	
	2 qubits	4 qubits	2 qubits	4 qubits
1	74.37%	85.10%	69.26%	85.12%
2	75.66%	85.27%	74.42%	83.75%
4	75.90%	83.98%	76.56%	82.30%
6	77.58%	84.54%	78.02%	85.31%
12	77.17%	85.52%	76.17%	85.70%

D. Recent hybrid QNN design used in topology optimization

We trained a NN with three layers of 150 neurons to perform PV topology reconfiguration in the classical system. In the hybrid QNN, we built several models and can compare some of them with the classical ones, as seen in Table 3.

TABLE 3 CLASSICAL AND QUANTUM TOPOLOGY RECONFIGURATION COMPARISON

Type	Qubit	Layers	Neuron vs gates	Epoch	Accuracy
Classical	N/A	3	150	150	~95%
Quantum	2	1	6	30	69.26%
Quantum	4	1	12	30	85.12%
Quantum	2	4	18	30	76.56%
Quantum	4	4	36	30	82.30%

As we see in Table 3, the quantum NN with four qubits is showing better results than the two qubit solution. With the classical NN having a test accuracy of approximately 95%, this hybrid QNN still shows promising results. This more recent hybrid QNN approach, based on circuit centric model [20], for topology optimization may still be improved upon. With these additional enhancements, we may bring the accuracy of proper selection to over 90%. With the simulation time and complexity of the circuit, a single-layer circuit may be sufficient for this type of dataset for initial testing. Further improvements to the four qubit, one-layer system will need further research. Future research will address exploring and studying quantum noise models with multiple Monte Carlo simulations and theoretical analysis.

IV. CONCLUSION

In this paper, we explored the use of QNN for topology reconfiguration in utility-scale PV arrays. The results from the QNN simulations for different numbers of qubits were presented. We observed that a QNN with only four qubits and one-layer gave promising results. Although, the classical NN provided a test accuracy of approximately 95%, the hybrid QNN achieved 85%. From sample simulation results and additional hyperparameter tuning it is anticipated that the QNN may achieve similar results. We have also tested a new circuit-centric model in the hybrid QNN which worked quite well. Future work will examine statistically different quantum noise models to reduce depolarization and dephasing errors [22], [23]. Adding a more accurate noise model will also better determine whether these hybrid QNN will run efficiently and accurately on current NISQ-era [24]–[26] quantum computers.

ACKNOWLEDGMENT

This research is supported in part by the NSF MRI Award number 2019068, the NSF I/UCRC award 1540040 and the Quantum Computing NCSS SenSIP I/UCRC project.

REFERENCES

- [1] S. Rao, S. Katoch, V. Narayanaswamy, G. Muniraju, C. Tepedelenlioglu, A. Spanias, P. Turaga, R. Ayyanar, and D. Srinivasan, "Machine Learning for Solar Array Monitoring, Optimization, and Control," *Synth. Lect. Power Electron.*, vol. 7, no. 1, pp. 1–91, Morgan and Claypool Publishers, 2020.
- [2] H. Braun, S. T. Buddha, V. Krishnan, A. Spanias, C. Tepedelenlioglu, T. Yeider, and T. Takehara, "Signal processing for fault detection in photovoltaic arrays," in *ICASSP, IEEE International Conference on Acoustics, Speech and Signal Processing - Proceedings*, 2012, pp. 1681–1684.
- [3] R. Fazai, K. Abodayeh, M. Mansouri, M. Trabelsi, H. Nounou, M. Nounou, and G. E. Georghiou, "Machine learning-based statistical testing hypothesis for fault detection in photovoltaic systems," *Sol. Energy*, vol. 190, pp. 405–413, 2019.
- [4] K. Jaskie, J. Martin, and A. Spanias, "PV Fault Detection Using Positive Unlabeled Learning," *Appl. Sci.*, vol. 11, no. 12, p. 5599, 2021.
- [5] H. Braun, S. T. Buddha, V. Krishnan, C. Tepedelenlioglu, A. Spanias, M. Banavar, and D. Srinivasan, "Topology reconfiguration for optimization of photovoltaic array output," *Sustain. Energy, Grids Networks*, vol. 6, pp. 58–69, 2016.
- [6] V. S. Narayanaswamy, R. Ayyanar, A. Spanias, C. Tepedelenlioglu, and D. Srinivasan, "Connection topology optimization in photovoltaic arrays using neural networks," in *Proceedings - 2019 IEEE International Conference on Industrial Cyber Physical Systems, IEEE ICPS 2019*, May 2019, pp. 167–172.
- [7] G. M. Tina, C. Ventura, S. Ferlito, and S. De Vito, "A state-of-art-review on machine-learning based methods for PV," *Applied Sciences (Switzerland)*, vol. 11, no. 16, p. 7550, 2021.
- [8] E. D. Chepp and A. Krenzinger, "A methodology for prediction and assessment of shading on PV systems," *Sol. Energy*, vol. 216, pp. 537–550, 2021.
- [9] G. Muniraju, S. Rao, S. Katoch, A. Spanias, C. Tepedelenlioglu, P. Turaga, M. K. Banavar, and D. Srinivasan, "A Cyber-Physical Photovoltaic Array Monitoring and Control System," *Int. J. Monit. Surveill. Technol. Res.*, vol. 5, no. 3, pp. 33–56, 2018.
- [10] S. Rao, D. Ramirez, H. Braun, J. Lee, C. Tepedelenlioglu, E. Kyriakides, D. Srinivasan, J. Frye, S. Koizumi, Y. Morimoto, and A. Spanias, "An 18 kW solar array research facility for fault detection experiments," *Proc. IEEE 18th MELECON*, Limassol, April 2016.
- [11] T. Takehara and S. Takada, "Photovoltaic panel monitoring apparatus," U.S. Patent 20110037600, Feb. 17, 2011.
- [12] A. S. Spanias, "Solar energy management as an Internet of Things (IoT) application," in *2017 8th International Conference on Information, Intelligence, Systems and Applications, IEEE IISA 2017*, Larnaca, Aug. 2017.
- [13] S. Rao, A. Spanias, and C. Tepedelenlioglu, "Solar array fault detection using neural networks," in *Proceedings - 2019 IEEE International Conference on Industrial Cyber Physical Systems, ICPS 2019*, 2019, pp. 196–200.
- [14] E. Garoudja, A. Chouder, K. Kara, and S. Silvestre, "An enhanced machine learning based approach for failures detection and diagnosis of PV systems," *Energy Convers. Manag.*, vol. 151, pp. 496–513, 2017.
- [15] J. P. Storey, P. R. Wilson, and D. Bagnall, "Improved optimization strategy for irradiance equalization in dynamic photovoltaic arrays," *IEEE Trans. Power Electron.*, vol. 28, no. 6, pp. 2946–2956, 2013.
- [16] M. Jazayeri, K. Jazayeri, and S. Uysal, "Adaptive photovoltaic array reconfiguration based on real cloud patterns to mitigate effects of non-uniform spatial irradiance profiles," *Sol. Energy*, vol. 155, pp. 506–516, 2017.
- [17] G. Uehara, S. Rao, M. Dobson, C. Tepedelenlioglu, and A. Spanias, "Quantum Neural Network Parameter Estimation for Photovoltaic Fault Detection," *IEEE IISA 2021*, July 2021.
- [18] Z. Jia, B. Yi, R. Zhai, Y. Wu, G. Guo, and G. Guo, "Quantum Neural Network States: A Brief Review of Methods and Applications," *Adv. Quantum Technol.*, vol. 2, no. 7–8, p. 1800077, 2019.
- [19] C. Cortes and V. Vapnik, "Support-vector networks," *Mach. Learn.*, vol. 20, no. 3, pp. 273–297, Sep. 1995.
- [20] M. Schuld, A. Bocharov, K. M. Svore, and N. Wiebe, "Circuit-centric quantum classifiers," *Phys. Rev. A*, vol. 101, no. 3, p. 32308, 2020.
- [21] V. Bergholm, J. Izaac, M. Schuld, C. Gogolin, M. S. Alam, S. Ahmed, J. M. Arrazola, C. Blank, A. Delgado, S. Jahangiri, K. McKiernan, J. J. Meyer, Z. Niu, A. Száva, and N. Killoran, "PennyLane: Automatic differentiation of hybrid quantum-classical computations," Nov. 2018.
- [22] J. Vovrosh, K. E. Khosla, S. Greenaway, C. Self, M. S. Kim, and J. Knolle, "Simple mitigation of global depolarizing errors in quantum simulations," *Phys. Rev. E*, vol. 104, no. 3, p. 035309, Sep. 2021.
- [23] L. M. Duan and G. C. Guo, "Reducing decoherence in quantum-computer memory with all quantum bits coupling to the same environment," *Phys. Rev. A - At. Mol. Opt. Phys.*, vol. 57, no. 2, pp. 737–741, Feb. 1998.
- [24] F. Leymann and J. Barzen, "The bitter truth about gate-based quantum algorithms in the NISQ era," *Quantum Sci. Technol.*, vol. 5, no. 4, 2020.
- [25] J. Preskill, "Quantum computing in the NISQ era and beyond," *Quantum*, vol. 2, 2018.
- [26] K. Bharti, A. Cervera-Lierta, T. H. Kyaw, T. Haug, S. Alperin-Lea, A. Anand, M. Degroote, H. Heimonen, J. S. Kottmann, T. Menke, W.-K. Mok, S. Sim, L.-C. Kwek, and A. Aspuru-Guzik, "Noisy intermediate-scale quantum (NISQ) algorithms," *arXiv*, pp. 1–82, 2021, [Online]. Available: <http://arxiv.org/abs/2101.08448>